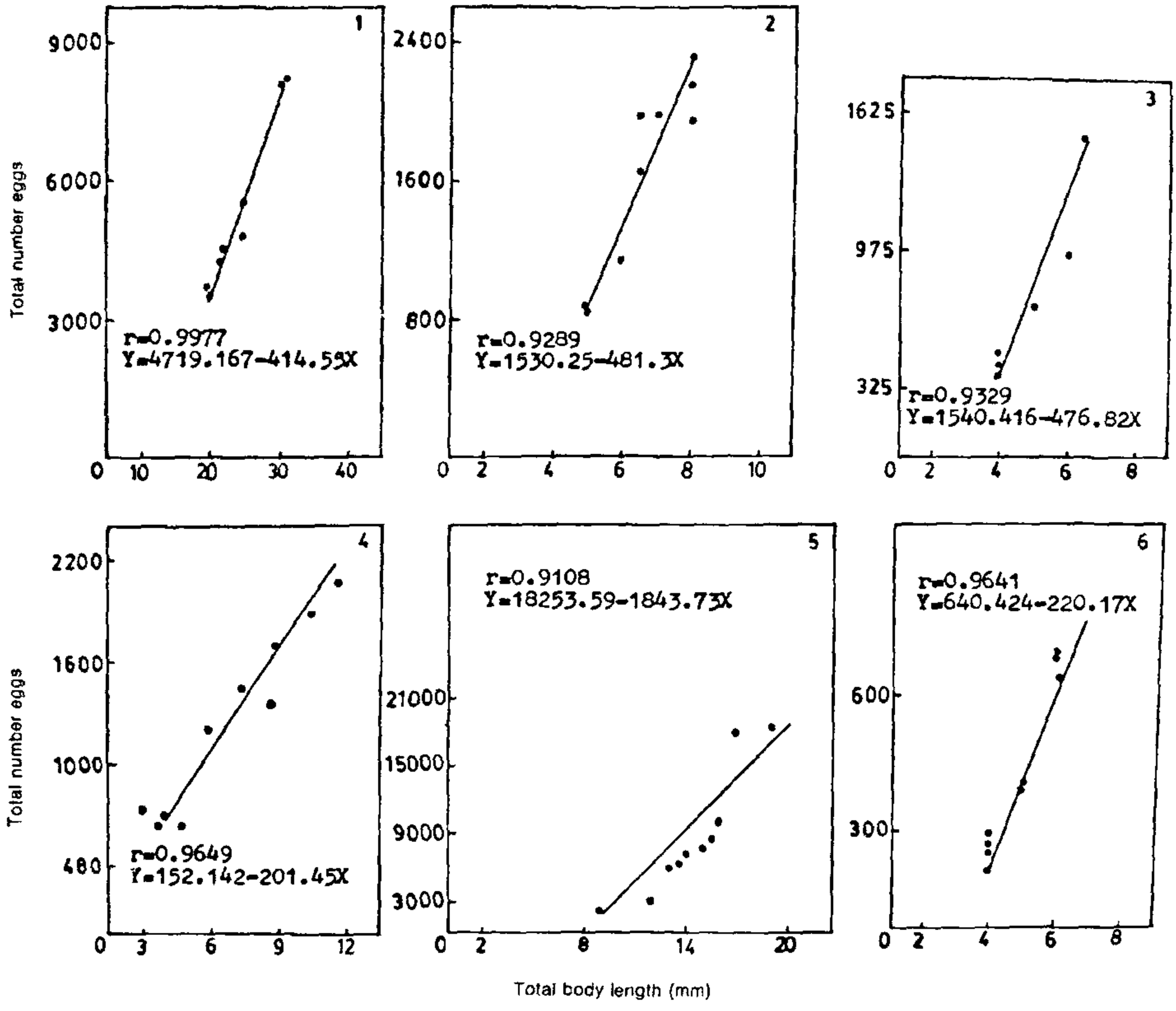

Figures 1–6. Correlation and regression values between the number of eggs and body length in **1,** Ephemeridae; **2,** Ephemerellidae; **3,** Caenidae; **4,** Leptophlebiidae; **5,** Heptageniidae; **6,** Baetidae.

The authors are grateful to Dr K. G. Sivaramakrishnan for valuable suggestions. Financial assistance from UGC, New Delhi, is gratefully acknowledged.

22 November 1988; Revised 4 March 1989

1. Clifford, H. F. and Boerger, H., *Can. Entomol.*, 1974, **106**, 1111.
2. Hunt, B. P., *Fla. Entomol.*, 1951, **34**, 59.
3. Britt, N. W., *Bull. Ohio. Biol. Surv.*, 1962, **1**, 70.
4. Clifford, H. F., *Can. J. Zool.*, 1970, **48**, 305.
5. Clifford, H. F., *Pan-Pac. Entomol.*, 1976, **52**, 265.
6. Minshall, J. D., *Am. Midl. Nat.*, 1967, **78**, 369.

CRYSTAL STRUCTURE OF PUTRESCINE–GLUTAMIC ACID COMPLEX

S. RAMASWAMY, M. NETHAJI* and M. R. N. MURTHY
*Molecular Biophysics Unit, *Inorganic and Physical Chemistry Department, Indian Institute of Science, Bangalore 560 012, India*

POLYAMINES are ubiquitous organic amines found in all living cells. Although their precise biological function is unknown, their importance in the life cycle of cells is reflected in the precise control mechanisms that have evolved to regulate polyamine

concentrations[1]. Polyamines increase during infection of cells by pathogens and also upon induction of cancer[1].

During studies on the biophysical properties of belladonna mottle virus (BDMV), it was observed that the virions contain polyamines that are essential for the integrity of virion particle structure. The polyamines are most probably bound to the viral nucleic acid[2]. Replacement of these intrinsic ions by monovalent cations such as sodium, potassium or lithium leads to loss of particle stability at alkaline pH[3].

These and several other observations[4] suggest that the mode of interaction between polyamines and nucleic acids cannot be modelled solely on the basis of electrostatic interactions. In order to understand the mode of interaction of polyamines with other biological molecules, and to explore the potential of these biogenic amines to adopt to a variety of chemical environments, we have initiated X-ray crystal structure studies of different polyamines crystallized in a variety of biologically relevant chemical contexts. The crystal structure of a complex between L-glutamic acid and putrescine is described in this communication.

Crystals of a 2:1 complex of L-glutamic acid and putrescine were obtained from an aqueous solution by liquid diffusion of propanol. The crystals belong to the monoclinic space group $P2_1$, with $a = 5.175$ Å, $b = 22.889$ Å, $c = 7.840$ Å and $\beta = 93.43°$. The calculated density based on 2 glutamic acid and 1 putrescine in the asymmetric unit is 1.3 g cm^{-3}.

X-ray diffraction data were collected on an Enraf Nonius 4 circle diffractometer using CAD4 geometry. X-rays from a microfocus sealed tube equipped with a molybdenum anode ($\lambda = 0.7107$ Å) were employed. A total of 1331 unique reflections were measured. The reflection intensities were corrected for Lorentz and polarization factors but not for absorption. During the data collection, standard reflections that were periodically monitored did not show any crystal decay.

The structure was solved by using the direct methods program MULTAN[5] and refined to an

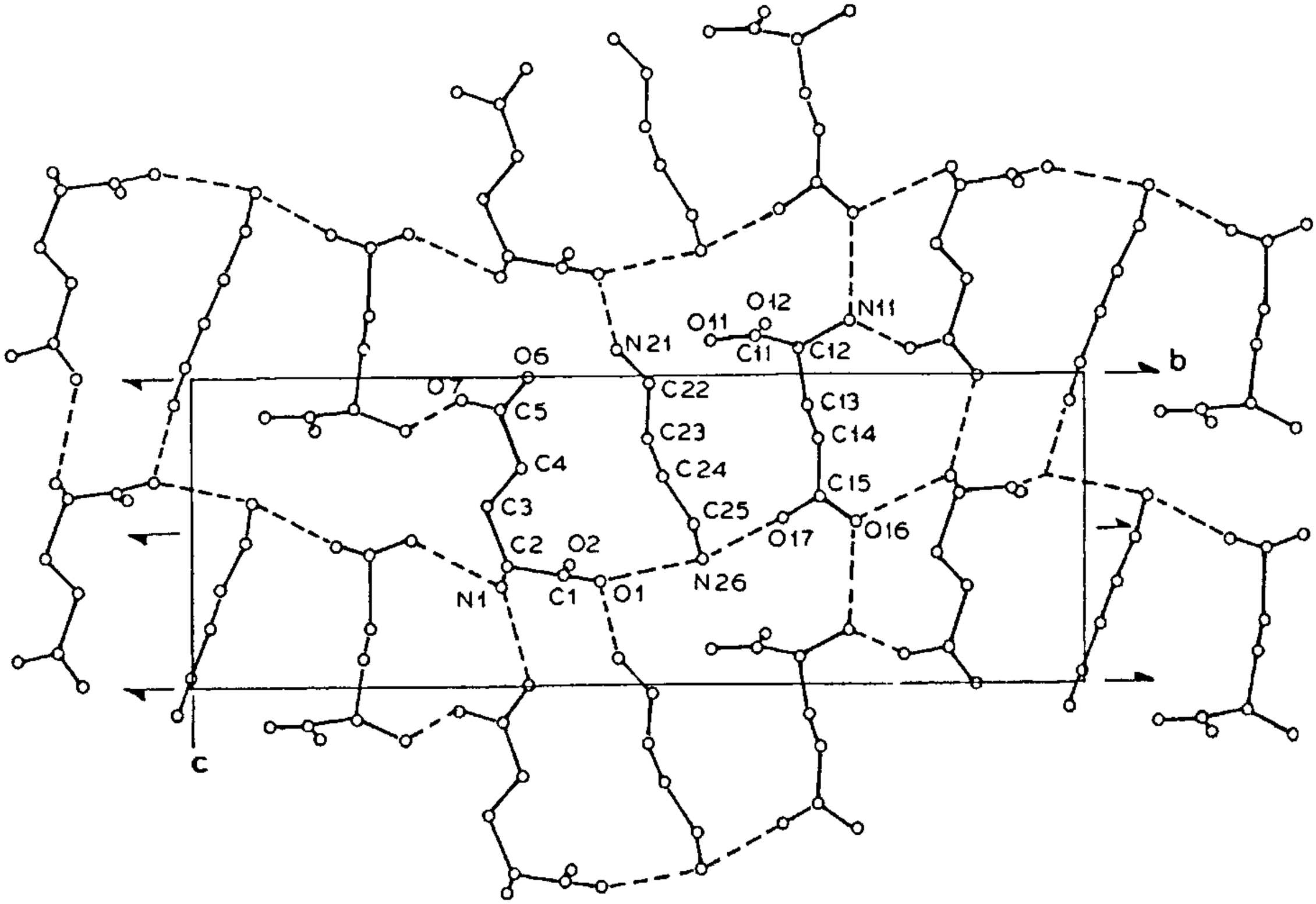

Figure 1. Projection of the structure of putrescine-glutamic acid complex on the *bc* plane.

Table 1 *Comparison of torsion angles of different glutamic acid forms*

Torsion angle (degrees)	α-form	β-form	Protonated form	Glu I	Glu II
N–C–C–O (1)	−50.2	−42.3	161.2	168.5	156 9
N–C–C–O (2)	130.3	141.2	−21 2	−10.9	−24.4
N–C–C–C	178.2	−51 8	−68.9	64.7	63.4
C–C–C–C	68.3	−73.1	−173.1	−179.6	174 8
C–C–C–O (6)	74.2	18.8	15.0	8.9	−53.0
C–C–C–O (7)	−104 6	−160.7	−167.0	−175.7	127.7

Glu I and Glu II are the two glutamic acid forms in the present structure.

$R = 5.1\%$ for reflections with $F_0 > 3\sigma(F_0)$, using a block diagonal structure factor least squares program. The calculations were performed on a DEC 1090 computer. During refinement the C, N, O atoms were refined with anisotropic temperature factors, whereas the hydrogens were associated with an isotropic temperature factor.

Examination of the final structure reveals that the two glutamic acid molecules in the asymmetric unit have two different conformations. Glutamic acid has been found to exist in α, β and a protonated form. In the α[6] and β[7] forms of L-glutamic acid, the α-carboxyl groups are protonated and a short hydrogen bond between the α-carboxyl and δ-carboxyl groups leads to a highly twisted side chain. In contrast, in the protonated form of L-glutamic acid hydrochloride[8], the side chain exists in an extended conformation. In the present case both carboxyls are charged and hence cannot be hydrogen-bonded amongst themselves. Accordingly the side chain conformation is closer, if not fully identical, to the protonated form. Table 1 lists the conformation angles of α, β and protonated forms of glutamic acid along with those of the two crystallographically independent glutamic acids in the present structure.

The glutamic acid amino groups hydrogen bond with both the main chain and side chain carboxyl groups. Table 2 gives a list of all the hydrogen bonding parameters. Figure 1 gives the projection of the packing diagram on the *bc* plane.

The conformation of putrescine in the complex is similar to those of its hydrochloride salts[9]. Table 3 gives the values of the conformational angles of putrescine from the two structures. It appears that the overriding influence in the crystal structure is the polyamine as the glutamic acid molecules have assumed conformations that are different from those found so far whereas the putrescine itself exists in its most favourable extended conformation. The observed molecular conformations satisfy the hydrogen bonding requirements of putrescine.

Table 2 *Hydrogen bonding pattern*

A	B	A–B length (Å)	H—A–B angle (degrees)	Symmetry
N1	06	2.7044	2.85	$x, y, z+1$
N1	02	2.8096	24.72	$x-1, y, z$
N1	016	2.7543	15.04	$-x, y-0.5, 1-z$
N11	07	2.8581	27.55	$1-x, y+0.5, -z$
N11	07	3.2964	20.73	$-x, y+0.5, -z$
N11	016	2.7882	10.54	$x, y, z-1$
N21	012	2.7048	8.17	$x+1, y, z$
N21	06	2.7619	13.16	$x+1, y, z$
N21	02	2.8042	5.18	$x, y, z-1$
N26	017	2.7708	10.40	x, y, z
N26	01	2.9585	4.45	x, y, z
N26	011	2.7737	20.38	$x+1, y, z+1$

Table 3 *Conformation angles of putrescine in the two structures*

Angle (degrees)	put . hcl	glu . put
N1–C1–C2–C3	−179.8	−177.1
C1–C2–C3–C4	−179.9	176.4
C2–C3–C4–N5	179.8	175.6

Thanks are due to Prof. H. Manohar, Department of Inorganic and Physical Chemistry, for diffractometer time. One of us (SR) is grateful to UGC, New Delhi, for a fellowship.

5 June 1989

1. Tabor, C. W. and Tabor, H., *Annu. Rev. Biochem.*, 1984, **53**, 749.
2. Savithri, H. S., Munshi, S. K., Suryanarayana, S., Divakar, S. and Murthy, M. R. N., *J. Gen. Virol.*, 1987, **68**, 1533.
3. Suryanarayana, S., Jacob, A. N. K. and Savithri,

H. S., *Indian J. Biochem. Biophys.*, 1988, **25,** 580.
4. Bartek-Wewiorowska, M. D. *et al., Int. J. Pure Appl. Chem.*, 1987, **59,** 407.
5. Main, P., Fiske, S. J., Hull, S. E., Lessinger, Germain, G., Deciercq, J. P. and Woolfson, M. M., *MULTAN 80 A system of computer programs for the automatic solution of crystal structures from X-ray diffraction data*, University of York, England, and Lourain, Belgium.
6. Lehmann, M. S. and Nunes, A. C., *Acta Crystallogr.*, 1980. **B36,** 1621.
7. Sakutaro Hirokawa, *Acta Crystallogr.*, 1955, **8,** 637.
8. Sequeira, A., Rajagopal, H. and Chidambaram, R., *Acta Crystallogr.*, 1972, **B28,** 2514.
9. Chandrasekar, K. and Vasantha Pattabhi, *Acta Crystallogr.*, 1980, **B36,** 2486.

A PRELIMINARY REPORT ON EARLY CELL TYPE-SPECIFIC ANTIBODIES IN *XENOPUS LAEVIS*

DEBJANI ROY
Institute of Self Organising Systems and Biophysics, North Eastern Hill University, Bijni Complex, Laitumukhrah, Shillong 793 003, India

IN recent years much work has been done to find biochemical markers of developmental stages. Amphibian embryos are a focus of attention[1-3] in these studies. Such markers are temporally or regionally restricted in early amphibian development[4,5].

There are still very few cell type markers for early amphibian embryos. The aim of the present investigation was to obtain monoclonal antibodies against early germ layer-specific antigens. The monoclonal antibody 3D7 recognizes an antigen that generally appears to be localized close to the cell membrane and also all over ectodermal cells in the early development of *Xenopus laevis*.

Embryos obtained via artificial fertilization by standard procedures were staged according to Nieuwkoop and Faber[6]. Embryos were dejellied in 2% cysteine hydrochloride (Sigma), pH 8.0, and then cultured in MMR (pH 7.8).

Monoclonal antibodies were raised against a crude cell homogenate from late blastula stage of *X. laevis* embryos. Immune mouse splenocytes were fused with Sp2/O-Ag14 myeloma cells[7] using published procedures[8]. Hybridomas that gave positive reaction were subcloned twice by limiting dilution. Screening of hybridoma supernatants was by ELISA using a cell homogenate from embryos at blastula stage. Colour development was measured at 492 nm in a Titertek Multiscan. Hybridomas that gave positive reaction were further tested by immunocytochemistry. Monoclonal antibody 3D7 was used in the study.

Embryos were fixed in 0.1% glutaraldehyde/2% paraformaldehyde for 6 h at room temperature. After fixation embryos were washed in PBS, dehydrated with ethanol, and embedded in paraffin. Sections were cut on a Spencer 820 (Lameris, Utrecht) microtome, collected and dried at 37°C for 24 h. Sections were deparaffinated with xylol and ethanol. Incubation with 3D7 ascites fluid (1:1000 dilution) for 60 min at 37°C was followed by 3 washes in PBS before incubation with a 1:50 dilution of goat anti-mouse IgM(Fc)–FITC (fluorescein isothiocyanate, Nordic) for 60 min at 37°C. Slides were washed with PBS, mounted in PBS–glycerol (1:1), and examined under a Leitz fluorescence microscope.

In control experiments, cryostat sections of unfixed or methanol-fixed embryos were used. Antibody localization was the same, but the quality of sections was poor and the background immunofluorescence high. Of all fixation procedures tried, the glutaraldehyde/formaldehyde fixation combined with paraffin embedding gave the best signal-to-background ratio.

The temporal and spatial pattern of 3D7 immunoreactivity analysed by immunocytochemistry shows many interesting features. In the unfertilized egg, the antigen is not localized but evenly distributed over the cytoplasm (figure 1, a). By 30 min post-fertilization, however, a striking redistribution of the antigen occurs (figure 1, b): the antigen becomes localized in a broad band in the periphery of the egg. In the cleavage stages, the antigen remains localized in the outer periphery of the cytoplasm (figure 1, c and d). When more cell layers develop, this outer-peripheral localization is restricted to the peripheral cell layer (figure 1, d). The intracellular localization is also restricted to the peripheral cell layers in the late blastula and early gastrula stages (figure 2, a). When the embryo gastrulates, the antigen become localized in the blastopore region,